
Fair GLASSO: Estimating Fair Graphical Models with Unbiased Statistical Behavior

Madeline Navarro
Rice University
nav@rice.edu

Samuel Rey
King Juan Carlos University
samuel.rey.escudero@urjc.es

Andrei Buciulea
King Juan Carlos University
andrei.buciulea@urjc.es

Antonio G. Marques
King Juan Carlos University
antonio.garcia.marques@urjc.es

Santiago Segarra
Rice University
segarra@rice.edu

Abstract

We propose estimating *Gaussian graphical models (GGMs)* that are *fair with respect to sensitive nodal attributes*. Many real-world models exhibit unfair discriminatory behavior due to biases in data. Such discrimination is known to be exacerbated when data is equipped with pairwise relationships encoded in a graph. Additionally, the effect of biased data on graphical models is largely underexplored. We thus introduce fairness for graphical models in the form of two bias metrics to promote balance in statistical similarities across nodal groups with different sensitive attributes. Leveraging these metrics, we present Fair GLASSO, a regularized graphical lasso approach to obtain sparse Gaussian precision matrices with unbiased statistical dependencies across groups. We also propose an efficient proximal gradient algorithm to obtain the estimates. Theoretically, we express the tradeoff between fair and accurate estimated precision matrices. Critically, this includes demonstrating when accuracy can be preserved in the presence of a fairness regularizer. On top of this, we study the complexity of Fair GLASSO and demonstrate that our algorithm enjoys a fast convergence rate. Our empirical validation includes synthetic and real-world simulations that illustrate the value and effectiveness of our proposed optimization problem and iterative algorithm.

1 Introduction

Data analysis frequently requires estimating complex dyadic relationships, which can be conveniently encoded in graphical representations such as Gaussian graphical models (GGMs) [1–3]. Myriad real-world applications model structure in data by obtaining graphs from observations, in fields including neuroscience, genomics, finance, and more [4–6]. However, it is known that real-world data can encode historical biases which models ought not to consider, such as discriminatory biases against sensitive populations [7, 8]. For example, social networks often exhibit preferential relationships that may unfairly discriminate against sensitive communities [9–11]. Moreover, the use of unfair graphs for downstream tasks is known to exacerbate existing biases [12–14]. While accurate graphical representations are critical for applications and analyses, the propagation of undesirable bias in graph data necessitates learning models that balance both fairness and accuracy.

The long-standing popularity of GGMs for several applications, many of them high-stakes, warrants care in how we estimate them from potentially biased data. However, there is no formal definition of fairness for graphical models, and existing definitions for graph-based machine learning may not be applicable for obtaining fair statistical relationships. Indeed, while fairness for graph data has recently received copious attention, the study of biased graphs in statistics and graph signal processing (GSP)

is only beginning [15–17]. Furthermore, previous works primarily consider fairness for downstream tasks, while few attempt to learn unbiased graphs from data [16–18]. We thus arrive at two vital questions. First, *what does it mean for a graphical model to be fair?* We aim to compare such a notion to existing definitions of fairness on graphs. Second, *how can we obtain GGMs that are fair in the presence of biased data?* To address these questions, we consider estimation of fair GGMs from biased observations, where nodes belong to groups corresponding to different sensitive attributes.

We propose an optimization framework to obtain fair GGMs from potentially biased data, where statistical dependencies between nodes show no preferences for particular groups. We first define fairness for graphical models by introducing two bias metrics that measure similarities in statistical behavior between pairs of groups. Our metrics are simple and convex, yet they intuitively capture biases in terms of conditional dependence. We then propose *Fair GLASSO*, a penalized maximum likelihood estimator using our bias metrics as regularizers, which aims to obtain sparse Gaussian precision matrices that optimally extract structural information from observed data while promoting fairer statistical behavior across node groups. We summarize our contributions as follows:

- We formally define fairness for graphical models via two bias metrics, one balancing statistical dependencies evenly across all groups and a stronger alternative requiring each node to be balanced across all groups. We relate our definition to other notions of fairness on graphs, where ours is specific to graphs encoding conditional dependence structures, which in turn allows greater interpretability and more detailed statistical analysis.
- We present *Fair GLASSO*, a penalized maximum likelihood estimator for sparse Gaussian precision matrices that are unbiased according to any measure of graphical fairness, which we demonstrate with our proposed bias metrics. We theoretically demonstrate that our approach yields a tradeoff between fairness and accuracy, which depends on the bias in the underlying graph.
- The convexity of Fair GLASSO under our proposed metrics allows us to propose an *efficient iterative method* based on proximal gradient descent. We show that our algorithm enjoys iterations of moderate complexity and provable convergence.
- We evaluate Fair GLASSO on both *synthetic and real-world datasets*. The former provides empirical validation of the efficiency of our algorithm and the existence of the fairness-accuracy tradeoff. The latter shows the myriad real-world applications for which we can reliably obtain graphical representations from data while also balancing statistical behavior across sensitive groups.

1.1 Notation

For any positive integer $p \in \mathbb{N}$, we let $[p] := \{1, 2, \dots, p\}$. For a matrix $\mathbf{X} \in \mathbb{R}^{p \times p}$ and a set of indices $\mathcal{C} \in [p]^2$, we let $\mathbf{X}_{\mathcal{C}}$ denote a masking operation on \mathbf{X} permitting non-zero entries only at indices in \mathcal{C} . If we define $\mathcal{D} := \{p(i-1) + i\}_{i=1}^p$, then $\mathbf{X}_{\mathcal{D}}$ is a diagonal matrix containing the diagonal entries of \mathbf{X} . For $\bar{\mathcal{D}} := [p]^2 \setminus \mathcal{D}$ denoting the complement of the set \mathcal{D} , $\mathbf{X}_{\bar{\mathcal{D}}} = \mathbf{X} - \mathbf{X}_{\mathcal{D}}$ contains non-zero values of \mathbf{X} only in its off-diagonal entries. We also let $\text{vec}(\mathbf{X}) \in \mathbb{R}^{p^2}$ denote the vertical concatenation of the columns of \mathbf{X} . The smallest and largest eigenvalues of a matrix \mathbf{X} are represented respectively by $\lambda_{\min}(\mathbf{X})$ and $\lambda_{\max}(\mathbf{X})$.

2 Fair Gaussian Graphical Models

GGMs succinctly model pairwise relationships in multivariate Gaussian distributions through intuitive graphical representations. We denote undirected graphs by $\mathcal{G} = (\mathcal{V}, \mathcal{E}, \mathbf{W})$, where $\mathcal{V} = [p]$ is the set of p nodes and $\mathcal{E} \subseteq \mathcal{V} \times \mathcal{V}$ the set of edges connecting pairs of nodes. For graphs with weighted edges, $\mathbf{W} \in \mathbb{R}^{p \times p}$ encodes the topological structure of \mathcal{G} such that $W_{ij} \neq 0$ if and only if $(i, j) \in \mathcal{E}$, that is, there is an edge in \mathcal{E} connecting nodes i and j with weight W_{ij} . Let $\mathbf{x} \in \mathbb{R}^p$ be a random vector following a zero-mean Gaussian distribution with positive definite covariance matrix $\Sigma_0 \succ 0$, that is, $\mathbf{x} \sim \mathcal{N}(\mathbf{0}, \Sigma_0)$. The precision matrix $\Theta_0 = \Sigma_0^{-1}$ completely describes the conditional dependence structure among the variables in \mathbf{x} . In particular, for any distinct pair $i, j \in [p]$, variables x_i and x_j are conditionally independent if and only if $[\Theta_0]_{ij} = 0$ [1, 2]. This Markovian property yields a graphical representation, where off-diagonal entries of Θ encode the weighted edges of a graph \mathcal{G} connecting conditionally dependent variables. In this work, we aim to obtain the structure encoded in Θ_0 using observations sampled from $\mathcal{N}(\mathbf{0}, \Sigma_0)$.

When considering group fairness, we associate each variable in \mathbf{x} with one of g groups that partition the variables according to a sensitive attribute [20, 21]. We represent group membership by the

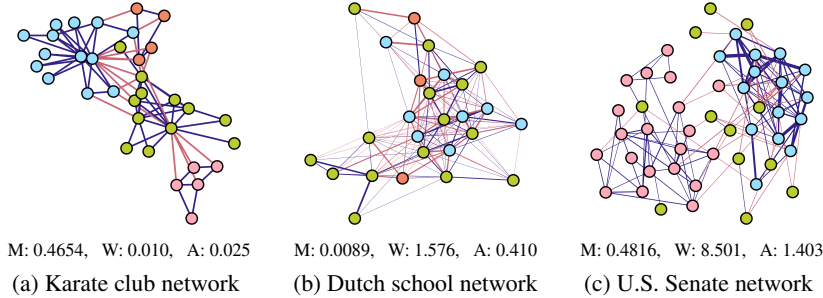


Figure 1: Three real-world networks with node groups denoted by color. Within-group edges are in blue and across-group edges in red, while edge widths correspond to edge weight magnitudes. For each network, we present (“M”) the modularity of the graphs with respect to group membership [19], (“W”) the ratio of positive to negative estimated partial correlations for within-group edges, and (“A”) an analogous ratio for across-group edges. Networks in (a) and (c) show high group-wise modularity, while (b) and (c) show significant preferences for positive correlations in the same group.

indicator matrix $\mathbf{Z} = [\mathbf{z}_1, \dots, \mathbf{z}_g] \in \{0, 1\}^{p \times g}$, where $Z_{ia} = 1$ if and only if variable i belongs to group $a \in [g]$, otherwise $Z_{ia} = 0$. Group sizes are denoted by $p_a = \sum_{i=1}^p Z_{ia}$ for every $a \in [g]$. We also assume that groups are non-overlapping, thus $p = \sum_{a=1}^g p_a$. GGMs may possess biases when a group of variables behaves significantly more or less similarly to particular groups. Indeed, individuals within the same political party tend to vote similarly [18]. In this case, entries of Θ_0 corresponding to pairs of voters of the same party will likely be positive and larger in magnitude.

We empirically demonstrate this phenomenon in Figure 1 for multiple real-world networks. Figures 1a and b show two social network examples, Zachary’s karate club network [22, 23] and the Dutch school network [24], where nodes represent individuals and edges connect them by their relationships. Figure 1c is a political network that connects U.S. senators if their voting patterns exhibit correlated behavior [18]. For each network, we present both their modularity with respect to group membership [19] and a comparison of their approximate partial correlations within and across nodal groups [25, 26]. Figures 1a and c show higher group-wise modularity, in line with the ubiquitous preference for within-group connections in real-world networks [9, 10]. However, observe that Figures 1b and c exhibit a clear preference for positive correlations between nodes in the same group. Despite its presence in real-world interconnected data, this type of discriminatory behavior is typically not addressed in existing works [27]. These examples inspire us to develop a definition of fairness for graphical models that accounts for both *correlation bias*, when behavior is highly correlated between certain groups, and *connectivity bias*, when connections are denser or sparser across certain group pairs.

2.1 Bias Metric for Fair Graphical Models

To address biases in both connectivity and correlations, we propose a definition of group fairness for graphical models. We consider the popular notion of demographic parity (DP), the primary choice for fairness on graphs [20]; however, other definitions of group fairness can be similarly adapted [21]. DP requires that outcomes be agnostic to sensitive attributes [20, 28]. In our case, we require estimation of graphical models with unbiased edge selection with respect to nodal groups. Thus, we present the following definition of dyadic DP for graphical models.

Definition 1 For a graphical model with the matrix $\Theta_0 \in \mathbb{R}^{p \times p}$ encoding the underlying conditional dependence structure, we consider DP to be satisfied if

$$\mathbb{P}[[\Theta_0]_{ij} | Z_{ia} = 1, Z_{ja} = 1] = \mathbb{P}[[\Theta_0]_{ij} | Z_{ia} = 1, Z_{jb} = 1] \quad \forall a, b \in [g]. \quad (1)$$

Note that the distribution need not be Gaussian for this definition. Intuitively, our graphical model DP requires that groups have evenly balanced connections across groups and do not behave significantly more or less similarly to certain groups. Crucially, Definition 1 accounts for both forms of bias showcased in Figure 1, *connectivity bias* in the support of Θ_0 and *correlation bias* in the signs of entries in Θ_0 . Not only is this definition appropriately tailored to fairness for graphical models, but it

also provides flexibility in how we address biases. We may adjust similarities in behavior without changing the topology of the graph [14, 29], but conversely, we may alter connections if correlations cannot be changed [30]. Finally, note that works for fairness on graphs with weighted or signed edges are rare [27], and to the best of our knowledge no previous work has specified fairness for graphical models that encode conditional dependencies.

We consider a graphical model unfair when there is a gap in DP, that is, when (1) does not hold. In practice, we measure biases in GGMs by approximating the DP gap. For this purpose, we propose the following bias metric,

$$H(\Theta) := \frac{1}{g^2 - g} \sum_{a=1}^g \sum_{b \neq a} \left(\frac{\mathbf{z}_a^\top \Theta_{\bar{D}} \mathbf{z}_a}{p_a^2 - p_a} - \frac{\mathbf{z}_a^\top \Theta_{\bar{D}} \mathbf{z}_b}{p_a p_b} \right)^2. \quad (2)$$

Each term in (2) compares the average within-group edge weight and the average across-group edge weight for every distinct group pair. Thus, $H(\Theta)$ will increase if variables belonging to two groups exhibit either significantly denser or sparser connections or significantly stronger or weaker correlations. As we aim to balance statistical behavior across groups, we consider obtaining precision matrices Θ that balance data fidelity with small values of $H(\Theta)$.

In addition to (2), we also propose a stronger alternative metric for node-wise fairness across groups,

$$H_{\text{node}}(\Theta) := \frac{1}{pg} \sum_{i=1}^p \sum_{a=1}^g \left(\frac{1}{g-1} \sum_{b \neq a} \frac{[\Theta_{\bar{D}} \mathbf{z}_a]_i}{p_a} - \frac{[\Theta_{\bar{D}} \mathbf{z}_b]_i}{p_b} \right)^2, \quad (3)$$

which is zero if and only if every variable is completely balanced across groups in terms of connections or correlation. As an alternative interpretation, observe that $H_{\text{node}}(\Theta)$ increases when the correlation between the group of a variable i and the i -th column of Θ increases [15, 18]. This node-wise penalty is stronger than $H(\Theta)$, as we require that not only pairs of groups exhibit no preference in statistical similarities but also each node must show no preference for connecting to certain groups.

3 Fair GLASSO

3.1 Graphical Lasso for Fair GGMs

We apply our proposed metrics in (2) and (3) to estimate GGMs from observations while mitigating both connectivity and correlation biases (see Section 2). Assume that we observe n samples from the distribution $\mathcal{N}(\mathbf{0}, \Sigma_0)$ collected in the data matrix $\mathbf{X} \in \mathbb{R}^{n \times p}$. To estimate fair and sparse precision matrices from data, we adapt the celebrated graphical lasso method [26, 31, 32], a penalized maximum likelihood approach for recovering GGMs.

Given the sample covariance matrix $\hat{\Sigma} = \frac{1}{n} \mathbf{X}^\top \mathbf{X}$, we present *Fair GLASSO*, a version of graphical lasso for fair GGMs,

$$\begin{aligned} \Theta^* &= \underset{\Theta}{\operatorname{argmin}} \operatorname{tr}(\hat{\Sigma} \Theta) - \log \det(\Theta + \epsilon \mathbf{I}) + \mu_1 \|\Theta_{\bar{D}}\|_1 + \mu_2 R_H(\Theta) \\ \text{s.t. } &\Theta \in \mathcal{M} := \{\Theta \in \mathbb{R}^{p \times p} : \Theta \succeq 0, \|\Theta\|_2^2 \leq \alpha\}, \end{aligned} \quad (4)$$

where R_H denotes a bias penalty measuring the fairness of Θ and $\mu_1, \mu_2 \geq 0$ tune the encouragement of sparse and fair precision matrices, respectively. For the penalty R_H , we can choose not only our proposed metrics H and H_{node} but also any metric for measuring bias on graphs. Similar to existing works on graph Laplacian GGMs [33], the addition of $\epsilon \mathbf{I}$ for $\epsilon > 0$ adds practicality to our approach, permitting us to obtain positive semi-definite precision matrices. The ability to estimate rank-deficient matrices allows for disconnected graph solutions. We assume that the true precision matrix Θ_0 has bounded eigenvalues (see AS2 and AS3 in Section 3.2), hence the constraint $\|\Theta\|_2^2 \leq \alpha$ on the spectral norm of Θ for large enough $\alpha > 0$. In practice, an effective α can be obtained by overshooting its value based on the minimum eigenvalue of the sample covariance $\hat{\Sigma}$. For further context of how both our proposed bias metrics H and H_{node} and our Fair GLASSO method relate to existing works, we provide a detailed review of related works in Appendix A.

3.2 Fair GLASSO Theoretical Analysis

We theoretically characterize the performance of Fair GLASSO. In particular, we focus on the effect of our fairness penalty in (4). Our result demonstrates the error rate of Θ^* not only from a traditional statistical perspective but also in terms of the bias in the true precision matrix Θ_0 . Indeed, as Θ_0 becomes more unfair, we expect that imposing unbiased estimates hinders estimation performance. Let the set $\mathcal{S} := \{(i, j) \in [p]^2 : [\Theta_0]_{ij} \neq 0, i \neq j\}$ contain the indices of the non-zero, off-diagonal entries of Θ_0 . We first share the following assumptions on Θ_0 and \mathbf{Z} .

AS1 (Bounded sparsity) There exists a constant $s > 0$ such that the cardinality of \mathcal{S} satisfies $|\mathcal{S}| \leq s$.

AS2 (Bounded spectrum) There exists a constant $\underline{k} > 0$ such that $\lambda_{\min}(\Sigma_0) \geq \underline{k} > 0$.

AS3 (Bounded spectrum) There exists a constant $\bar{k} > 0$ such that $\lambda_{\max}(\Sigma_0) \leq \bar{k} < \infty$.

AS4 (Persistent groups) All groups have the same size, that is, $p_a = \bar{p} \geq 2$ for every $a \in [g]$.

Assumptions AS1, AS2, and AS3 follow those from the distinguished work [32]. Note that AS4 is imposed for simplicity, but similar results hold if we merely require asymptotically similar groups sizes, where no groups vanish as $p \rightarrow \infty$. With our assumptions in place, we present our main result on the error rate of Fair GLASSO, the proof of which can be found in Appendix B.

Theorem 1 Assume that AS1 to AS4 hold and that $\mu_1 \asymp \sqrt{(\log p)/n}$ and $\mu_2 = o(1)$. Moreover, let $R_H = H$ from (2) and $\epsilon = 0$ in (4). With probability tending to 1 as $p \rightarrow \infty$, there exist constants $m_1, m_2 > 0$ such that

$$\|\Theta^* - \Theta_0\|_F \leq m_1 \sqrt{\frac{(p+s)\log p}{n}} + m_2 \frac{\sqrt{g} \sqrt[4]{H(\Theta_0)}}{\sqrt{p}}. \quad (5)$$

Moreover, there exists a constant $q > 0$ such that if μ_2 satisfies

$$\mu_2^2 \leq \frac{qp^2 \log p}{g^2 n \sqrt{H(\Theta_0)}}, \quad (6)$$

then with probability tending to 1 as $p \rightarrow \infty$ we can further guarantee that

$$\|\Theta^* - \Theta_0\|_F \leq m_1 \sqrt{\frac{(p+s)\log p}{n}}. \quad (7)$$

Our error bound consists of the Frobenius norm convergence rate for graphical lasso in [32] and a term accounting for the bias penalty in (4). In particular, the second term in (5) portrays the influence of bias in the true precision matrix Θ_0 . Theorem 1 not only provides an intuitive error bound for fair estimation of GGMs but also exemplifies when a tradeoff between fairness and accuracy may occur. When the true model Θ_0 is biased, that is, $H(\Theta_0)$ is large, then performance may suffer according to (5). However, if bias mitigation is mild enough, that is, if μ_2 is small enough to satisfy (6), then we instead enjoy the error rate of [32] with no adverse effect from the bias penalty. Indeed, as the true Θ_0 becomes fairer, so too grows the range of values of μ_2 that guarantee (7). Thus, if Θ_0 is unbiased, then imposing a strong bias penalty can obtain fair estimates Θ^* while maintaining accuracy.

In addition to the explicit Frobenius error rate of Θ^* , we are also interested in when we can sufficiently describe the true model behavior. Our next result shows how well Fair GLASSO solutions approximate the true distribution, which enjoys the same rate as in Theorem 1, proven in Appendix C.

Corollary 1 Let the assumptions of Theorem 1 hold. Then, with probability tending to 1 as $p \rightarrow \infty$, there exist constants $m'_1, m'_2 > 0$ such that

$$\|\Theta^* \Sigma_0 - \mathbf{I}\|_F \leq m'_1 \sqrt{\frac{(p+s)\log p}{n}} + m'_2 \frac{\sqrt{g} \sqrt[4]{H(\Theta_0)}}{\sqrt{p}}. \quad (8)$$

Moreover, there exists a constant $q > 0$ such that when μ_2 satisfies (6), then with probability tending to 1 as $p \rightarrow \infty$ we can further guarantee that

$$\|\Theta^* \Sigma_0 - \mathbf{I}\|_F \leq m'_1 \sqrt{\frac{(p+s)\log p}{n}}. \quad (9)$$

Note that a similar rate to (9) holds up to a constant if we replace Σ_0 with $\hat{\Sigma}$. Thus, we may apply $\|\Theta^* \hat{\Sigma} - \mathbf{I}\|_F$ as an error metric when the true covariance matrix Σ_0 is unavailable.

3.3 Algorithmic Implementation

If we choose R_H in (4) as H or H_{node} , the convexity of the resultant problem allows us to introduce a simple yet effective algorithm for Fair GLASSO estimates. We base our approach on an accelerated proximal gradient method known as fast iterative shrinkage algorithm (FISTA) [34], which is well suited to solving non-smooth, constrained optimization problems.

Algorithm 1: Fair GLASSO from Gaussian observations.

Input: Sample covariance $\hat{\Sigma}$, weights μ_1 and μ_2 , Lipschitz constant L of f .

- 1 Initialize $\hat{\Theta}^{(0)} = \check{\Theta}^{(1)} \in \mathcal{M}$, $t^{(1)} = 1$, $k = 1$.
- 2 **while** *Stopping criteria not met* **do**
- 3 Proximal gradient descent: $\check{\Theta}^{(k)} = \mathcal{T}_{\mu_1/L} \left(\hat{\Theta}^{(k-1)} - \frac{1}{L} \nabla f(\hat{\Theta}^{(k-1)}) \right)$.
- 4 Projection step: $\hat{\Theta}^{(k)} = \Pi_{\mathcal{M}}(\check{\Theta}^{(k)})$.
- 5 Adaptive step size update: $t^{(k+1)} = \frac{1}{2} (1 + \sqrt{1 + 4(t^{(k)})^2})$.
- 6 Accelerated update: $\check{\Theta}^{(k+1)} = \hat{\Theta}^{(k)} + \frac{t^{(k)} - 1}{t^{(k+1)}} (\hat{\Theta}^{(k)} - \hat{\Theta}^{(k-1)})$.
- 7 Update iteration: $k = k + 1$.
- 8 **end**

Output: Estimated precision matrix $\hat{\Theta} = \hat{\Theta}^{(k)}$.

We separate the Fair GLASSO objective function $F(\Theta) = f(\Theta) + h(\Theta)$ into its smooth and non-smooth terms via $f(\Theta)$ and $h(\Theta)$, respectively, which are given by

$$f(\Theta) := \text{tr}(\hat{\Sigma}\Theta) - \log \det(\Theta + \epsilon \mathbf{I}) + \mu_2 R_H(\Theta), \quad h(\Theta) := \mu_1 \|\Theta_{\mathcal{D}}\|_1. \quad (10)$$

The proposed algorithm to estimate Θ^* is presented in Algorithm 1. We discuss the steps of our algorithm in Appendix D, and we provide further details in Appendix E, including specifying the gradient $\nabla_{\Theta} f$ and the Lipschitz constant of f when $R_H = H$ or $R_H = H_{\text{node}}$.

Computationally, the complexity of Algorithm 1 is limited by an eigendecomposition in the projection step and a matrix inverse in the proximal gradient descent step (see (28) and (29) in Appendix D for details). Over-the-shelf implementations of these operations render a computational complexity of $\mathcal{O}(p^3)$. However, implementations based on fast matrix multiplication may result in an improved complexity of $\mathcal{O}(p^{2.4})$, a remarkable improvement since the optimization problem involves learning p^2 variables. Finally, in addition to a mild computational complexity, the proposed algorithm enjoys a convergence rate of $\mathcal{O}(\frac{1}{k^2})$, which we formally state next and prove in Appendix F.

Theorem 2 *Let $\{\hat{\Theta}^{(k)}\}_{k \geq 1}$ be the sequence generated by Algorithm 1 for solving the optimization problem (4), where we denote the global minimum by Θ^* . Then, for any $k \geq 1$,*

$$\|\hat{\Theta}^{(k)} - \Theta^*\|_F^2 \leq \frac{4L \|\Theta^{(0)} - \Theta^*\|_F^2}{\alpha(k+1)^2}, \quad (11)$$

where L is the Lipschitz constant of $f(\Theta)$ and α corresponds to the spectral constraint in (4).

Thus, Theorem 2 guarantees convergence of Algorithm 1 to the optimal solution Θ^* under our constraints in (4) with either of our bias metrics in (2) or (3).

4 Experiments

We illustrate the ability of Fair GLASSO to reliably estimate both synthetic and real-world graphs from data while promoting unbiased connections. Extensive experimental details including our performance metrics, the baselines with which we compare, and the real-world datasets are provided in Appendix G; these details are summarized here.

We compare our method with existing approaches for both scalability and performance. In particular, we consider (i) **GL**: Traditional graphical lasso [26], (ii) **FGL**: Fair GLASSO with $R_H = H$, (iii) **NFGL**: Fair GLASSO with $R_H = H_{\text{node}}$, (iv) **FST**: Network inference from spectral templates with a group-wise bias penalty [18, 35], (v) **NFST**: Network inference from spectral templates with a node-wise bias penalty [15, 18], and (vi) **RWGL**: Graphical lasso with randomly rewired edges.

We then perform GGM estimation on multiple real-world networks: (i) **Karate club**: the social network of Zachary’s karate club members [23], (ii) **School**: A contact network of high school

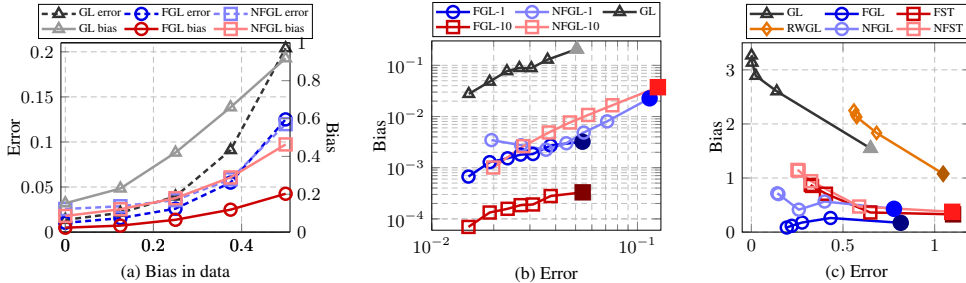


Figure 2: Estimation performance in terms of error and bias. (a) Bias and error for estimating a fair graph as data becomes more biased. (b) Bias and error as graph size p grows for ER graphs. (c) Bias and error for a biased real-world network [23] as the number of observations n grows.

students [36], (iii) **Friendship**: The friendship network of the same high school students as in School [36], (iv) **Co-authorship**: An author collaboration network [37], and (v) **MovieLens**: A movie recommender network [38]. Figure 1 demonstrated that interconnected data may have fair or unfair relationships; thus, our experiment not only exemplifies the viability of our approach for real-world settings but also the fairness-accuracy tradeoff depending on biases in data.

4.1 Estimating Fair Graphs with Biased Data

Consider the realistic setting where our model is to be implemented in a fair setting, but our observations contain unfair biases [8]. We aim to obtain accurate graphical models by reducing the biases encoded in data. We consider synthetic networks whose nodes show no preferential connections, but our observations become increasingly unfair, growing in preference for within-group correlations.

Figure 2a presents the error and bias from networks estimated using graphical lasso with and without bias penalties H and H_{node} . As expected, all methods show an increase in both error and bias as the data becomes more unfair, as our observations are not only straying from the true distribution but also tending toward unfair behavior. However, **FGL** and **NFGL** not only preserve a lower bias than **GL**, but we also improve estimation performance. This significant result exemplifies the situation described in Section 3.2; our proposed penalties not only yield unbiased estimates but also serve as informative priors when the underlying graph is fair. Thus, we enjoy improvement in both fairness and accuracy for this realistic setting.

4.2 Performance as Graph Size Increases

Fair GLASSO adapts traditional GGM learning through the bias penalty, which includes (2) and (3). To observe the regularization effect of our penalties, we compare graphical lasso both with and without bias penalties for estimating synthetic networks as the graph size p grows, which also demonstrates the scalability of our method. We thus implement **GL** via a state-of-the-art approach for comparison [26].

Figure 2b shows the relationship between error and bias in the estimated graphs. Each line corresponds to a graph estimation method, and points on the lines denote the varying dimension, ranging from $p = 50$ (highlighted via darker, filled markers) to $p = 1000$.

First, observe that **GL** achieves superior accuracy at the expense of a larger bias, while **NFGL** improves bias, albeit with greater error. In contrast, **FGL** for $\mu_2 \in \{1, 10\}$ can improve bias without sacrificing accuracy, where $\mu_2 = 10$ yields the most Pareto-optimal solution. This result aligns with Theorem 1, showcasing the ability of Fair GLASSO to maintain estimation performance while significantly improving the fairness of the obtained graph. Critically, even as p increases, our method enjoys relatively short running times, ranging from 0.5 seconds for 50 nodes to 30 minutes for 1000, which we show in Table 1. Our implementation of the classical algorithm in [26] requires 2 seconds and 170 minutes for $p = 50$ and $p = 1000$, respectively. We can then conclude that our efficient algorithm for Fair GLASSO can sufficiently handle larger graphs.

Nodes p	GL	FGL-0	FGL-1
50	2.06	0.55	0.64
200	18.80	8.14	8.87
1000	10225.74	1900.89	1893.57

Table 1: Running time in seconds of Algorithm 1 and graphical lasso via [26].

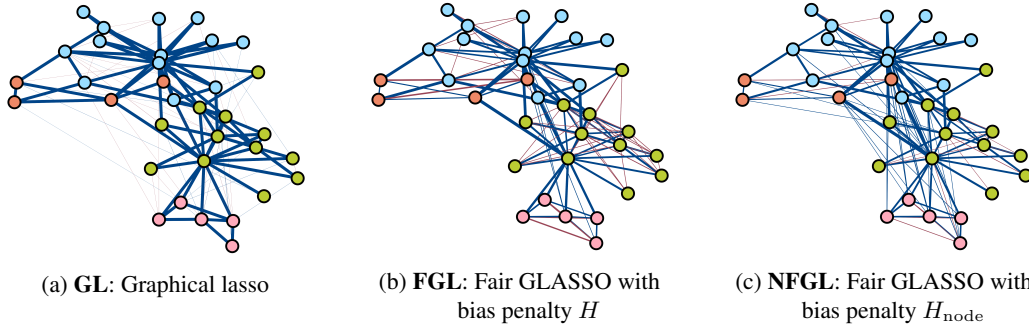


Figure 3: Estimated **Karate club** network via graphical lasso with and without penalties H and H_{node} . Node colors denote group membership, while edge thickness denotes edge weight magnitude and edge color its sign, with blue (red) as positive (negative) correlation. (a) Estimation via **GL**. (b) Estimation via **FGL**. (c) Estimation via **NFGL**.

4.3 Social Network with Synthetic Signals

We next apply Fair GLASSO for the **Karate club** network, a real-world graph with known biased connections [23]. As this network famously exhibits group-wise modularity [22], we can compare different methods for estimating a real biased network. We show bias and error as the number of data samples increases from $n = 10^2$ (denoted by darker, filled markers) to $n = 10^5$ in Figure 2c. Since this graph does not have data, we generate synthetic Gaussian observations on the social network.

For all methods, increasing the number of samples improves estimation error, but bias also grows since the underlying graph is unfair. Observe that all alternatives to **GL** are able to reduce estimation bias. As expected, randomly rewiring edges from graphical lasso estimates in **RWGL** does mildly improve bias when compared to **GL**, but error also rises significantly. The methods designed for fair graph estimation achieve the greatest improvement in bias, with our proposed methods **FGL** and **NFGL** outperforming **FST** and **NFST** in both bias and error. Moreover, not only does **FGL** outperform other methods in both fairness and accuracy for all n , but **FGL** is the only approach that simultaneously decreases bias and error. Fair GLASSO is therefore viable for estimating real-world networks with known biased connections.

We also investigate the effect of H versus H_{node} for estimating group-wise modular networks. Figure 3 visualizes three graphs learned using **GL**, **FGL**, and **NFGL**. Both **FGL** and **NFGL** attempt to mitigate biased connections by reducing larger weights for existing within-group edges. However, since **FGL** aims to improve bias in expectation, Figure 3b shows an increase in negative within-group edges, that is, negative partial correlations between nodes in the same group. Conversely, Figure 3c shows a network with more balanced connections *per node*, where more nodes are connected to new edges that are both positive and negative. This result suggests that the bias metric H for group-wise balance in expectation aligns more with existing definitions of DP, while the node-wise DP gap H_{node} behaves closer to an individual fairness metric [39, 40].

4.4 Fair GGMs for Real-World Data

Finally, in Table 2 we evaluate Fair GLASSO to estimate graphs from four real-world datasets consisting of two social networks, **School** and **Friendship** with *gender* as the sensitive attribute; a collaboration network **Co-authorship** with groups representing the *type of conference* in which each author publishes most; and a recommendation network **MovieLens**, where we consider binary sensitive attributes for each movie (node) denoting whether or not the movie was *released after 1991*. As each network varies in level of biases in their connections and observations, we show results for both weak and strong bias mitigation, that is, $\mu_2 \in \{1, 10^6\}$, for all fair graph learning methods.

For the relatively unbiased **School** and **Friendship** networks, our methods **FGL** and **NFGL** obtain superior estimation accuracy while sufficiently accounting for biases, particularly in comparison with **FST** and **NFST**. Unsurprisingly, we observe the lowest estimation error when $\mu_2 = 1$ is small enough such that **FGL** and **NFGL** achieve similar bias to **Ground truth**. However, observe that **FGL** and **NFGL** have low estimation error even for large $\mu_2 = 10^6$, which enjoys significant bias reduction.

	School		Co-authorship		MovieLens		Friendship	
	Error	Bias	Error	Bias	Error	Bias	Error	Bias
Ground truth	–	0.2030	–	14.052	–	0.6791	–	0.1487
GL	0.2661	0.3111	0.1995	12.6102	0.0223	0.9529	0.6477	0.4068
RWGL-150	0.3497	0.3943	0.2308	12.5836	2.1919	0.9409	0.6509	0.4068
RWGL-300	0.3775	0.5110	0.2978	12.5735	2.2002	0.9184	0.6633	0.3861
FST ($\mu_2 = 1$)	0.4383	0.8942	0.4188	0.5754	0.1724	4.0568	1.0606	0.3787
NFST ($\mu_2 = 1$)	0.4386	0.8924	0.4068	6.6887	0.1724	4.0568	1.1149	0.3734
FST ($\mu_2 = 10^6$)	1.7820	1.0767	1.0801	129.5384	0.1724	4.0568	1.1924	0.0052
NFST ($\mu_2 = 10^6$)	1.6131	3.1971	1.0500	176.6285	0.1724	4.0568	1.1852	0.0081
FGL ($\mu_2 = 1$)	0.1417	0.4824	0.1896	10.3317	0.0253	0.8177	0.0505	0.1657
NFGL ($\mu_2 = 1$)	0.1417	0.4824	0.1895	11.8391	0.0253	0.8177	0.0505	0.1657
FGL ($\mu_2 = 10^6$)	0.1449	0.0308	0.2432	0.1899	0.0248	0.6106	0.0516	0.0153
NFGL ($\mu_2 = 10^6$)	0.2981	0.0827	0.2708	0.7908	0.0239	0.7104	0.0873	0.0243

Table 2: Bias and error for estimating four real-world networks. The top row shows the bias present in the true underlying network. The best performances are in **bold**.

This verifies the results from Theorem 1 and in Figure 2a for real-world data; when the underlying graph is fair, our bias penalties serve as informative structural priors that improve performance.

For the **Co-authorship** network, we also observe the best accuracy using **FGL** and **NFGL** when μ_2 is small enough that bias is similar to that of the true network. Critically, even when μ_2 is large, we observe errors for **FGL** and **NFGL** competitive with **GL** while also achieving low bias. Moreover, for the **MovieLens** dataset, Fair GLASSO is the only method that rivals **GL** in accuracy while acquiring significantly fairer estimates. Indeed, **FGL** with $\mu_2 = 10^6$ is the only method to achieve both low error and bias simultaneously. This implies that the observations in both the **Co-authorship** and **MovieLens** datasets are biased, since high bias mitigation yielding fair estimates improves estimation performance. Thus, we demonstrate that relationships in real data can be explained by graphical models rivaling the accuracy of state-of-the-art approaches while also exhibiting fairer behavior.

5 Conclusion

This work proposes two metrics to evaluate bias in graphical models, which we apply as regularizers for fair GGM estimation. In particular, we adapt DP to measure biases in the conditional dependence structure encoded in graphical models, where nodes may show preferences for certain groups in terms of either connections or correlations. Unlike existing works that typically only consider fairness based on the unweighted topology of a known graph, we extend the concept of graph DP for the weighted connectivity patterns represented by the precision matrix of a Gaussian distribution. Moreover, we apply our group fairness for graphical models to modify graphical lasso for estimating fair GGMs. Future work will see more general graphical models, along with other extensions both in terms of the graph setting and fairness, which we discuss further in Appendix H.

Broader Impact

In this work, we proposed a fair adaptation of graphical lasso, an extremely prominent method for complex data analysis. The development of methods that encourage fairness is necessary to ensure ethical and trustworthy tools, particularly those applied as extensively as GGMs to several critical and sensitive applications. Our paper contributes to expanding available unbiased graph-based methods, leading to extensions of other graphical models and statistical tools.

Moreover, as fairness on graphs is still nascent, several graph-based tasks have yet to be considered under the lens of fairness. Indeed, models are typically encouraged to be unbiased with respect to independent entities, but recent years have seen greater attention paid to the treatment of data equipped with graphical relationships. We not only participate in this movement, but we also extend fairness on graphs by considering weighted and signed edges for graphical models encoding conditional dependencies. This paper serves as a critical step in developing fair graph-based tools, particularly as GGMs are used in several high-stakes fields, including finance and medicine.

References

- [1] Daphne Koller and Nir Friedman. *Probabilistic graphical models: Principles and techniques*. MIT press, 2009.
- [2] Steffen L Lauritzen. *Graphical models*, volume 17. Clarendon Press, 1996.
- [3] Gonzalo Mateos, Santiago Segarra, Antonio G. Marques, and Alejandro Ribeiro. Connecting the dots: Identifying network structure via graph signal processing. *IEEE Signal Processing Magazine*, 36(3):16–43, 2019.
- [4] Eugene Belilovsky, Gaël Varoquaux, and Matthew B Blaschko. Testing for differences in gaussian graphical models: Applications to brain connectivity. In *Advances in Neural Information Processing Systems*, volume 29, 2016.
- [5] Stephen M. Smith, Karla L. Miller, Gholamreza Salimi-Khorshidi, Matthew Webster, Christian F. Beckmann, Thomas E. Nichols, Joseph D. Ramsey, and Mark W. Woolrich. Network modelling methods for FMRI. *NeuroImage*, 54(2):875–891, 2011.
- [6] Oliver Stegle, Sarah A. Teichmann, and John C. Marioni. Computational and analytical challenges in single-cell transcriptomics. *Nature Reviews Genetics*, 16(3):133–145, 2015.
- [7] Cynthia Dwork, Moritz Hardt, Toniann Pitassi, Omer Reingold, and Richard Zemel. Fairness through awareness. In *Innovations in Theoretical Computer Science*, page 214–226, 2012.
- [8] Anja Lambrecht and Catherine Tucker. Algorithmic bias? an empirical study of apparent gender-based discrimination in the display of STEM career ads. *Management Science*, 65(7):2966–2981, 2019.
- [9] Fariba Karimi, Mathieu Génois, Claudia Wagner, Philipp Singer, and Markus Strohmaier. Homophily influences ranking of minorities in social networks. *Scientific Reports*, 8(1):11077, 2018.
- [10] Yosh Halberstam and Brian Knight. Homophily, group size, and the diffusion of political information in social networks: Evidence from Twitter. *Journal of Public Economics*, 143:73–88, 2016.
- [11] Eli Pariser. *The filter bubble: How the new personalized web is changing what we read and how we think*. Penguin, 2011.
- [12] Avishek Bose and William Hamilton. Compositional fairness constraints for graph embeddings. In *International Conference on Machine Learning*, volume 97, pages 715–724, 2019.
- [13] Enyan Dai and Suhang Wang. Say no to the discrimination: Learning fair graph neural networks with limited sensitive attribute information. In *International Conference on Web Search and Data Mining*, page 680–688, 2021.
- [14] Peizhao Li, Yifei Wang, Han Zhao, Pengyu Hong, and Hongfu Liu. On dyadic fairness: Exploring and mitigating bias in graph connections. In *International Conference on Learning Representations*, 2021.
- [15] O. Deniz Kose, Yanning Shen, and Gonzalo Mateos. Fairness-aware optimal graph filter design. *arXiv preprint arXiv:2310.14432*, 2023.
- [16] Davoud Ataee Tarzanagh, Laura Balzano, and Alfred O. Hero. Fair community detection and structure learning in heterogeneous graphical models. *arXiv preprint arXiv:2112.05128*, 2023.
- [17] Xiang Zhang and Qiao Wang. A unified framework for fair spectral clustering with effective graph learning. *arXiv preprint arXiv:2311.13766*, 2023.
- [18] Madeline Navarro, Samuel Rey, Andrei Buciualea, Antonio G Marques, and Santiago Segarra. Mitigating subpopulation bias for fair network topology inference. *arXiv preprint arXiv:2403.15591*, 2024.
- [19] Farzan Masrour, Tyler Wilson, Heng Yan, Pang-Ning Tan, and Abdol Esfahanian. Bursting the filter bubble: Fairness-aware network link prediction. *AAAI Conference on Artificial Intelligence*, 34(01):841–848, 2020.
- [20] Michael Feldman, Sorelle A. Friedler, John Moeller, Carlos Scheidegger, and Suresh Venkatasubramanian. Certifying and removing disparate impact. In *ACM International Conference on Knowledge Discovery and Data Mining*, page 259–268, 2015.
- [21] Moritz Hardt, Eric Price, Eric Price, and Nati Srebro. Equality of opportunity in supervised learning. In *Advances in Neural Information Processing Systems*, volume 29, 2016.

- [22] M. Girvan and M. E. J. Newman. Community structure in social and biological networks. *Proceedings of the National Academy of Sciences of the United States of America*, 99(12):7821–7826, 2002.
- [23] Wayne W. Zachary. An information flow model for conflict and fission in small groups. *Journal of Anthropological Research*, 33(4):452–473, 1977.
- [24] Andrea Beate Knecht. *Friendship selection and friends’ influence: dynamics of networks and actor attributes in early adolescence*. PhD thesis, University Utrecht, 2008.
- [25] A. P. Dempster. Covariance selection. *Biometrics*, 28(1):157–175, 1972.
- [26] Jerome Friedman, Trevor Hastie, and Robert Tibshirani. Sparse inverse covariance estimation with the graphical lasso. *Biostatistics*, 9(3):432–441, 2008.
- [27] Akрати Saxena, George Fletcher, and Mykola Pechenizkiy. FairSNA: Algorithmic fairness in social network analysis. *ACM Computing Surveys*, 56(8):1–45, 2024.
- [28] Michael Kearns, Seth Neel, Aaron Roth, and Zhiwei Steven Wu. Preventing fairness gerrymandering: Auditing and learning for subgroup fairness. In *International Conference on Machine Learning*, volume 80, pages 2564–2572, 2018.
- [29] Indro Spinelli, Simone Scardapane, Amir Hussain, and Aurelio Uncini. FairDrop: Biased edge dropout for enhancing fairness in graph representation learning. *IEEE Transactions on Artificial Intelligence*, 3(3): 344–354, 2022.
- [30] Oyku Deniz Kose and Yanning Shen. Fair contrastive learning on graphs. *IEEE Transactions on Signal and Information Processing over Networks*, 8:475–488, 2022.
- [31] Alexandre d’Aspremont, Onureena Banerjee, and Laurent El Ghaoui. First-order methods for sparse covariance selection. *SIAM Journal on Matrix Analysis and Applications*, 30(1):56–66, 2008.
- [32] Adam J. Rothman, Peter J. Bickel, Elizaveta Levina, and Ji Zhu. Sparse permutation invariant covariance estimation. *Electronic Journal of Statistics*, 2, 2008.
- [33] Jiayi Ying, José Vinícius de Miranda Cardoso, and Daniel Palomar. Nonconvex sparse graph learning under Laplacian constrained graphical model. In *Advances in Neural Information Processing Systems*, volume 33, pages 7101–7113, 2020.
- [34] Amir Beck and Marc Teboulle. A fast iterative shrinkage-thresholding algorithm for linear inverse problems. *SIAM J. Imaging Sciences*, 2(1):183–202, 2009.
- [35] Santiago Segarra, Antonio G. Marques, Gonzalo Mateos, and Alejandro Ribeiro. Network topology inference from spectral templates. *IEEE Transactions on Signal and Information Processing over Networks*, 3(3):467–483, 2017.
- [36] Julie Fournet and Alain Barrat. Contact patterns among high school students. *PLoS ONE*, 9(9):e107878, 2014.
- [37] Andrei Buciualea, Elvin Isufi, Geert Leus, and Antonio G Marques. Learning graphs and simplicial complexes from data. In *IEEE International Conference on Acoustics, Speech, and Signal Processing*, pages 9861–9865, 2024.
- [38] F. Maxwell Harper and Joseph A. Konstan. The MovieLens datasets: History and context. *ACM Trans. Interact. Intell. Syst.*, 5(4), 2015.
- [39] Yushun Dong, Jian Kang, Hanghang Tong, and Jundong Li. Individual fairness for graph neural networks: A ranking based approach. In *ACM International Conference on Knowledge Discovery and Data Mining*, pages 300–310, 2021.
- [40] Jian Kang, Jingrui He, Ross Maciejewski, and Hanghang Tong. InFoRM: Individual fairness on graph mining. In *ACM International Conference on Knowledge Discovery and Data Mining*, pages 379–389, 2020.
- [41] Eric D Kolaczyk. *Statistical analysis of network data: Methods and models*. Springer, 2009.
- [42] Brian Baingana, Gonzalo Mateos, and Georgios B. Giannakis. Proximal-gradient algorithms for tracking cascades over social networks. *IEEE Journal of Selected Topics in Signal Processing*, 8(4):563–575, 2014.

- [43] Onureena Banerjee, Laurent El Ghaoui, and Alexandre d’Aspremont. Model selection through sparse maximum likelihood estimation for multivariate Gaussian or binary data. *Journal of Machine Learning Research*, 9(15):485–516, 2008.
- [44] Jianqing Fan and Runze Li. Variable selection via nonconcave penalized likelihood and its oracle properties. *Journal of the American Statistical Association*, 96(456):1348–1360, 2001.
- [45] Cun-Hui Zhang. Nearly unbiased variable selection under minimax concave penalty. *The Annals of Statistics*, 38(2):894–942, 2010.
- [46] Samuel Rey, Madeline Navarro, Andrei Buciualea, Santiago Segarra, and Antonio G Marques. Joint graph learning from gaussian observations in the presence of hidden nodes. In *Asilomar Conference on Signals, Systems, and Computers*, pages 53–57. IEEE, 2022.
- [47] Patrick Danaher, Pei Wang, and Daniela M. Witten. The joint graphical lasso for inverse covariance estimation across multiple classes. *Journal of the Royal Statistical Society, Series B (Statistical Methodology)*, 76(2):373–397, 2013.
- [48] Andrei Buciualea, Jiayi Ying, Antonio G Marques, and Daniel P Palomar. Polynomial graphical lasso: Learning edges from gaussian graph-stationary signals. *arXiv preprint arXiv:2404.02621*, 2024.
- [49] Nicolai Meinshausen and Peter Bühlmann. High-dimensional graphs and variable selection with the Lasso. *The Annals of Statistics*, 34(3), 2006. ISSN 0090-5364.
- [50] Pradeep Ravikumar, Martin J. Wainwright, Garvesh Raskutti, and Bin Yu. High-dimensional covariance estimation by minimizing ℓ_1 -penalized log-determinant divergence. *Electronic Journal of Statistics*, 5, 2011. ISSN 1935-7524.
- [51] Clifford Lam and Jianqing Fan. Sparsistency and rates of convergence in large covariance matrix estimation. *The Annals of Statistics*, 37(6B), 2009.
- [52] Pradeep Ravikumar, Martin J. Wainwright, and John D. Lafferty. High-dimensional Ising model selection using ℓ_1 -regularized logistic regression. *The Annals of Statistics*, 38(3), 2010. ISSN 0090-5364.
- [53] Eunho Yang, Genevera Allen, Zhandong Liu, and Pradeep Ravikumar. Graphical models via generalized linear models. In *Advances in Neural Information Processing Systems*, volume 25, 2012.
- [54] Rebecca Morrison, Ricardo Baptista, and Youssef Marzouk. Beyond normality: Learning sparse probabilistic graphical models in the non-Gaussian setting. In *Advances in Neural Information Processing Systems*, volume 30, 2017.
- [55] Sandeep Kumar, Jiayi Ying, Jose Vinicius de Miranda Cardoso, and Daniel Palomar. Structured graph learning via Laplacian spectral constraints. In *Advances in Neural Information Processing Systems*, volume 32, 2019.
- [56] Madeline Navarro, Samuel Rey, Andrei Buciualea, Antonio G Marques, and Santiago Segarra. Joint network topology inference in the presence of hidden nodes. *IEEE Transactions on Signal Processing*, 2024.
- [57] Samuel Rey, T. Mitchell Roddenberry, Santiago Segarra, and Antonio G. Marques. Enhanced graph-learning schemes driven by similar distributions of motifs. *IEEE Transactions on Signal Processing*, 71: 3014–3027, 2023.
- [58] Martín Sevilla, Antonio G. Marques, and Santiago Segarra. Estimation of partially known Gaussian graphical models with score-based structural priors. In *International Conference on Artificial Intelligence and Statistics*, pages 1558–1566, 2024.
- [59] Ruijia Wang, Xiao Wang, Chuan Shi, and Le Song. Uncovering the structural fairness in graph contrastive learning. In *Advances in Neural Information Processing Systems*, volume 35, pages 32465–32473, 2022.
- [60] Maarten Buyl and Tijn De Bie. DeBayes: A Bayesian method for debiasing network embeddings. In *International Conference on Machine Learning*, volume 119, pages 1220–1229, 2020.
- [61] Le Wu, Lei Chen, Pengyang Shao, Richang Hong, Xiting Wang, and Meng Wang. Learning fair representations for recommendation: A graph-based perspective. In *ACM Web Conference*, pages 2198–2208, 2021.
- [62] Chirag Agarwal, Himabindu Lakkaraju, and Marinka Zitnik. Towards a unified framework for fair and stable graph representation learning. In *The Conference on Uncertainty in Artificial Intelligence*, volume 161, pages 2114–2124, 2021.

- [63] O. Deniz Kose and Yanning Shen. Fair node representation learning via adaptive data augmentation. *arXiv:2201.08549*, 2022.
- [64] Yushun Dong, Ninghao Liu, Brian Jalaian, and Jundong Li. EDITS: Modeling and mitigating data bias for graph neural networks. In *ACM Web Conference*, pages 1259–1269, 2022.
- [65] O. Deniz Kose and Yanning Shen. FairWire: Fair graph generation. *arXiv:2402.04383*, 2024.
- [66] Peter J. Bickel and Elizaveta Levina. Regularized estimation of large covariance matrices. *The Annals of Statistics*, 36(1):199–227, 2008.
- [67] Amir Beck. *First-order methods in optimization*. SIAM, 2017.

A Related Work

A.1 Graph Estimation

Obtaining graphical representations from data has long stood as one of the most prominent tasks in several fields, including statistics, GSP, and more [3, 41, 42]. Maximum likelihood estimation of GGMs was first introduced by Dempster [25], and subsequent additions of the ℓ_1 -norm penalty produced the famous graphical lasso approach [31, 32, 43]. Several modifications and extensions followed, typically proposing alternative penalties [4, 44–48], and its popularity has brought about copious theoretical investigation into its performance, its limitations, and more [26, 32, 49–51]. While Gaussianity is typical for estimating graphs, extensions to non-Gaussian distributions are also well studied [52–54]. Similar approaches have found use in GSP, both under additional constraints and in more general settings [33, 35, 55, 56].

Most works learn graphs from data solely to preserve some notion of fidelity that may potentially be aided by prior structural assumptions [57, 58]. However, estimating graphs while improving performance in both accuracy and fairness in connections remains novel [18]. Moreover, to the best of our knowledge, we are the first to estimate graphical models from data while explicitly encouraging fairness in its connections, particularly in terms of both connectivity and correlation bias [16].

A.2 Fairness on Graphs

Fairness in graph-based tasks has received much attention recently, particularly in the field of machine learning. In addition to group fairness [13, 14], some works consider other definitions such as individual or structural fairness [39, 40, 59]. The most prevalent tasks for fairness on graphs are link prediction [12, 14, 19, 60, 61] and node representation [12, 13, 61–63], where nodes must experience equal treatment regardless of their sensitive attributes. Some works directly alter graph structure to promote unbiased connections, but, unlike our work, this requires a known graph [14, 19, 29, 30, 60, 64].

A number of works consider creating fair graphs, which share our goal of obtaining graph representations that possess unbiased connectivity patterns [16–18, 65]. This includes fair graph generative models [65], which aims to learn distributions of graph data, whereas we learn graph structure from nodal observations. We note [16–18] as the only other works of which we are aware that estimate graphs from data while considering fair outcomes. However, for [16, 17], the task is fundamentally different as they aim to cluster nodes fairly without explicitly imposing fairness on graph structure. While the task in [18] is the same as ours, we differ not only in how our samples are modeled but also in our definition of fairness, which is specific to graphical models encoding conditional dependence. Moreover, we provide further theoretical results, including guarantees of both error rates and algorithmic convergence.

B Proof of Theorem 1

Our proof of Theorem 1 is inspired by that of [32]. We first require the following lemma [66, Lemma A.3], which allows us to bound differences between entries of estimated and true Gaussian covariance matrix entries with high probability.

Lemma 1 (Bickel and Levina [66]) *For iid Gaussian random vectors $\mathbf{Z}_i \sim \mathcal{N}(\mathbf{0}, \mathbf{S})$ for $i \in [n]$ such that $\lambda_{\max}(\mathbf{S}) \leq \bar{k} < \infty$, we have that*

$$\mathbb{P} \left[\left| \sum_{\ell=1}^n Z_{i\ell} Z_{j\ell} - S_{ij} \right| \geq n\epsilon \right] \leq c_1 \exp\{-c_2 n\epsilon^2\},$$

where $\epsilon > 0$ is bounded, and c_1 , c_2 , and ϵ are dependent only on \bar{k} .

We proceed with the proof of (5) in the statement of Theorem 1. Consider a function Q that measures the difference in the objective of (4) given $\Theta \in \mathcal{M}$ and the true precision matrix Θ_0 ,

$$\begin{aligned} Q(\Theta) &:= \text{tr}(\hat{\Sigma}\Theta) - \log \det \Theta + \mu_1 \|\Theta_{\mathcal{D}}\|_1 + \mu_2 H(\Theta) \\ &\quad - \text{tr}(\hat{\Sigma}\Theta_0) + \log \det \Theta_0 - \mu_1 \|[\Theta_0]_{\mathcal{D}}\|_1 - \mu_2 H(\Theta_0) \\ &= \text{tr}((\hat{\Sigma} - \Sigma_0)(\Theta - \Theta_0)) + \text{tr}(\Sigma_0(\Theta - \Theta_0)) - (\log \det \Theta - \log \det \Theta_0) \\ &\quad + \mu_1 (\|\Theta_{\mathcal{D}}\|_1 - \|[\Theta_0]_{\mathcal{D}}\|_1) + \mu_2 (H(\Theta) - H(\Theta_0)). \end{aligned}$$

We may also represent the objective difference in terms of the disparity between Θ and Θ_0 , that is, $G(\Delta) = Q(\Theta_0 + \Delta)$ for $\Delta = \Theta - \Theta_0$, where we have

$$\begin{aligned} G(\Delta) &= \text{tr}((\hat{\Sigma} - \Sigma_0)\Delta) + \text{tr}(\Sigma_0\Delta) - (\log \det(\Theta_0 + \Delta) - \log \det \Theta_0) \\ &\quad + \mu_1 (\|(\Theta_0 + \Delta)_{\mathcal{D}}\|_1 - \|[\Theta_0]_{\mathcal{D}}\|_1) + \mu_2 (H(\Theta_0 + \Delta) - H(\Theta_0)). \end{aligned} \quad (12)$$

We may then use Q and G to compare Θ^* and Θ_0 via their difference under the objective function of our proposed graphical lasso problem (4).

By the definition of $\Theta^* \in \mathcal{M}$ as the minimizer of (4), we have that $Q(\Theta^*) \leq 0$ and thus $G(\Delta^*) \leq 0$ for $\Delta^* = \Theta^* - \Theta_0$. If we can show that $G(\Delta) > 0$ for every $\Delta \in \mathcal{M}$ such that

$$\|\Delta\|_F > m_1 r_n + m_2 \frac{g^4 \sqrt{H(\Theta_0)}}{\sqrt{p}} \quad (13)$$

where

$$r_n := \sqrt{\frac{(p+s)\log p}{n}}$$

for some constants $m_1, m_2 > 0$, then we know that $\|\Delta^*\|_F$ satisfies (5) in Theorem 1, as desired. To this end, we obtain a lower bound of $G(\Delta)$ and determine the conditions under which we can guarantee that $G(\Delta) > 0$ for any $\Delta \in \mathcal{M}$ such that (13) holds.

Trace difference. We begin by addressing the first term of (12). By the triangle inequality, we define nonnegative values t_1 and t_2 such that

$$\left| \text{tr}((\hat{\Sigma} - \Sigma_0)\Delta) \right| \leq \left| \sum_{i \neq j} (\hat{\Sigma}_{ij} - [\Sigma_0]_{ij}) \Delta_{ij} \right| + \left| \sum_{i=1}^p (\hat{\Sigma}_{ii} - [\Sigma_0]_{ii}) \Delta_{ii} \right| =: t_1 + t_2,$$

for which we provide an upper bound. To bound t_1 , note that by Lemma 1, we may choose any constant $c_1 > 0$ such that

$$|\hat{\Sigma}_{ij} - [\Sigma_0]_{ij}| = \left| \frac{1}{n} \sum_{k=1}^n X_{ki} X_{kj} - [\Sigma_0]_{ij} \right| \geq c_1 \sqrt{\frac{\log p}{n}}$$

with probability at most $d_1 p^{-d_2 c_1^2}$ for constants $d_1, d_2 > 0$. Then, by the union sum inequality,

$$\begin{aligned} \mathbb{P} \left[\max_{i \neq j} |\hat{\Sigma}_{ij} - [\Sigma_0]_{ij}| \geq c_1 \sqrt{\frac{\log p}{n}} \right] &= \mathbb{P} \left[\bigcup_{i \neq j} |\hat{\Sigma}_{ij} - [\Sigma_0]_{ij}| \geq c_1 \sqrt{\frac{\log p}{n}} \right] \\ &\leq \sum_{i \neq j} \mathbb{P} \left[|\hat{\Sigma}_{ij} - [\Sigma_0]_{ij}| \geq c_1 \sqrt{\frac{\log p}{n}} \right] \\ &\leq d_1 (p^2 - p) p^{-d_2 c_1^2} \leq d_1 p^{-d_3}, \end{aligned} \quad (14)$$

where $c_1 > \sqrt{2/d_2}$ and $d_3 > d_2 c_1^2 - 2$. We then apply the Cauchy-Schwarz inequality for the following bound on t_1 ,

$$t_1 \leq \max_{i \neq j} |\hat{\Sigma}_{ij} - [\Sigma_0]_{ij}| \cdot \|\Delta_{\mathcal{D}}\|_1 \leq c_1 \sqrt{\frac{\log p}{n}} \|\Delta_{\mathcal{D}}\|_1, \quad (15)$$

whose probability tends to 1 as $p \rightarrow \infty$ as in the right-hand side of (14).

For t_2 , we again apply the Cauchy-Schwarz inequality and Lemma 1 to obtain

$$\begin{aligned}
t_2 &\leq \left(\sum_{i=1}^p (\hat{\Sigma}_{ii} - [\Sigma_0]_{ii})^2 \right)^{1/2} \cdot \|\Delta_{\mathcal{D}}\|_F \\
&\leq \sqrt{p} \max_{i \in [p]} |\hat{\Sigma}_{ii} - [\Sigma_0]_{ii}| \cdot \|\Delta_{\mathcal{D}}\|_F \\
&\leq c_2 \sqrt{\frac{p \log p}{n}} \cdot \|\Delta_{\mathcal{D}}\|_F \\
&\leq c_2 r_n \|\Delta_{\mathcal{D}}\|_F
\end{aligned} \tag{16}$$

with probability again approaching 1 as $p \rightarrow \infty$.

We combine (15) and (16) to obtain a lower bound of the first term of (12),

$$\text{tr}((\hat{\Sigma} - \Sigma_0)\Delta) \geq - \left| \text{tr}((\hat{\Sigma} - \Sigma_0)\Delta) \right| \geq -c_1 \sqrt{\frac{\log p}{n}} \|\Delta_{\bar{\mathcal{D}}}\|_1 - c_2 r_n \|\Delta_{\mathcal{D}}\|_F. \tag{17}$$

Log-determinant difference. We next consider the difference of log determinants in $G(\Delta)$. Consider the function $f(t) = \log \det(\Theta_0 + t\Delta)$. The derivative and second derivative of $f(t)$ are

$$\begin{aligned}
f'(t) &= \text{tr}((\Theta_0 + t\Delta)^{-1}\Delta), \\
f''(t) &= -\text{tr}(\Delta(\Theta_0 + t\Delta)^{-1}\Delta(\Theta_0 + t\Delta)^{-1}),
\end{aligned}$$

respectively. Then, the Maclaurin series expansion of $f(1)$ with the integral form of the remainder is

$$f(1) - f(0) = f'(0) + \int_0^1 f''(v)(1-v)dv,$$

so by the symmetry of Θ_0 and Δ we apply the Kronecker product for

$$\begin{aligned}
&\log \det(\Theta_0 + \Delta) - \log \det \Theta_0 \\
&= \text{tr}(\Sigma_0\Delta) - \int_0^1 (1-v) \text{tr}(\Delta(\Theta_0 + v\Delta)^{-1}\Delta(\Theta_0 + v\Delta)^{-1})dv \\
&= \text{tr}(\Sigma_0\Delta) - \text{vec}(\Delta)^\top \left[\int_0^1 (1-v)(\Theta_0 + v\Delta)^{-1} \otimes (\Theta_0 + v\Delta)^{-1} dv \right] \text{vec}(\Delta).
\end{aligned}$$

Recall that the definition of the smallest eigenvalue of a matrix \mathbf{A} is $\lambda_{\min}(\mathbf{A}) = \min_{\mathbf{x}: \|\mathbf{x}\|_2=1} \mathbf{x}^\top \mathbf{A} \mathbf{x}$. We thus have

$$\begin{aligned}
&\log \det(\Theta_0 + \Delta) - \log \det \Theta_0 \\
&\leq \text{tr}(\Sigma_0\Delta) - \|\Delta\|_F^2 \lambda_{\min} \left(\int_0^1 (1-v)(\Theta_0 + v\Delta)^{-1} \otimes (\Theta_0 + v\Delta)^{-1} dv \right) \\
&\leq \text{tr}(\Sigma_0\Delta) - \|\Delta\|_F^2 \int_0^1 (1-v) \lambda_{\min}^2(\Theta_0 + v\Delta)^{-1} dv
\end{aligned}$$

since the eigenvalues of the Kronecker product of two matrices are the products of their eigenvalues. Then, we have that

$$\begin{aligned}
\log \det(\Theta_0 + \Delta) - \log \det \Theta_0 &\leq \text{tr}(\Sigma_0\Delta) - \frac{1}{2} \|\Delta\|_F^2 \min_{v \in [0,1]} \lambda_{\min}^2(\Theta_0 + v\Delta)^{-1} \\
&\leq \text{tr}(\Sigma_0\Delta) - \frac{1}{2} \|\Delta\|_F^2 \lambda_{\min}^2(\Theta_0 + \Delta)^{-1} \\
&= \text{tr}(\Sigma_0\Delta) - \frac{1}{2} \|\Delta\|_F^2 \lambda_{\max}^{-2}(\Theta_0 + \Delta) \\
&\leq \text{tr}(\Sigma_0\Delta) - \frac{1}{2} \|\Delta\|_F^2 (\|\Theta_0\|_2 + \|\Delta\|_2)^{-2} \\
&\leq \text{tr}(\Sigma_0\Delta) - \frac{1}{2} \|\Delta\|_F^2 (\underline{k}^{-1} + \|\Delta\|_F)^{-2}.
\end{aligned}$$

We define $\tau := \max\{4, (1 + \underline{k} \|\Delta\|_F)^2\}$, which gives us

$$\begin{aligned} \log \det(\Theta_0 + \Delta) - \log \det \Theta_0 &\leq \text{tr}(\Sigma_0 \Delta) - \frac{1}{2} \|\Delta\|_F^2 (\underline{k}^{-1} \max\{2, \underline{k} \|\Delta\|_F + 1\})^{-2} \\ &\leq \text{tr}(\Sigma_0 \Delta) - \frac{1}{2\tau} \underline{k}^2 \|\Delta\|_F^2. \end{aligned} \quad (18)$$

Sparsity penalties. For the sparsity penalties, note that by the definition of \mathcal{S} , $\|[\Theta_0 + \Delta]_{\mathcal{D}}\|_1 = \|[\Theta_0 + \Delta]_{\mathcal{D} \cap \mathcal{S}}\|_1 + \|\Delta_{\mathcal{D} \cap \mathcal{S}^c}\|_1$ and $\|[\Theta_0]_{\mathcal{D}}\|_1 = \|[\Theta_0]_{\mathcal{D} \cap \mathcal{S}}\|_1$. Then, by the triangle inequality,

$$\mu_1 (\|[\Theta_0 + \Delta]_{\mathcal{D}}\|_1 - \|[\Theta_0]_{\mathcal{D}}\|_1) \geq \mu_1 (\|\Delta_{\mathcal{D} \cap \mathcal{S}^c}\|_1 - \|\Delta_{\mathcal{D} \cap \mathcal{S}}\|_1). \quad (19)$$

DP gaps. Finally, we consider the difference in DP gaps. Observe that $H(\Theta)$ is both differentiable and convex in Θ . Thus, we have that

$$\begin{aligned} H(\Theta_0 + \Delta) - H(\Theta_0) &\geq \text{tr}(\nabla_{\Theta} H(\Theta_0) \Delta) \\ &\geq - |\text{tr}(\nabla_{\Theta} H(\Theta_0) \Delta)| \\ &\geq - |\text{tr}(\nabla_{\Theta} H(\Theta_0) \Theta_0)| - |\text{tr}(\nabla_{\Theta} H(\Theta_0) \Theta)| \\ &\geq - \|\nabla_{\Theta} H(\Theta_0)\|_* (\|\Theta_0\|_2 + \|\Theta\|_2) \\ &\geq - (\alpha^{1/2} + \underline{k}^{-1}) \|\nabla_{\Theta} H(\Theta_0)\|_*. \end{aligned}$$

Moreover, recall that by definition \mathbf{C}_{ab} is block-wise constant for every $a, b \in [g]$. Thus, the gradient $\nabla_{\Theta} H(\Theta_0)$ as in the right-hand side of (29) is block-wise constant with g blocks, hence it is at most rank g . We then have that

$$\begin{aligned} \|\nabla_{\Theta} H(\Theta_0)\|_* &\leq \sqrt{g} \|\nabla_{\Theta} H(\Theta_0)\|_F \\ &\leq \frac{2\sqrt{g}}{g^2 - g} \sum_{a=1}^g \sum_{b \neq a} \text{tr}(\mathbf{C}_{ab} \Theta_0) \|\mathbf{C}_{ab}\|_F \\ &= \frac{2\sqrt{g}}{g^2 - g} \sum_{a=1}^g \sum_{b \neq a} |\text{tr}(\mathbf{C}_{ab} \Theta_0)| \left(\frac{1}{\bar{p}^2 - \bar{p}} + \frac{1}{\bar{p}^2} \right)^{1/2} \\ &\leq \frac{4\sqrt{g}}{\bar{p}(g^2 - g)} \sum_{a=1}^g \sum_{b \neq a} |\text{tr}(\mathbf{C}_{ab} \Theta_0)| \\ &\leq \frac{4\sqrt{g}}{\bar{p}\sqrt{g^2 - g}} \left(\sum_{a=1}^g \sum_{b \neq a} |\text{tr}(\mathbf{C}_{ab} \Theta_0)|^2 \right)^{1/2}, \end{aligned}$$

where the last inequality holds by $\|\mathbf{x}\|_1 \leq \sqrt{m} \|\mathbf{x}\|_2$ for any vector $\mathbf{x} \in \mathbb{R}^m$. By the definition of H ,

$$\|\nabla_{\Theta} H(\Theta_0)\|_* \leq \frac{4\sqrt{g}}{\bar{p}} \sqrt{H(\Theta_0)}.$$

We then have the following lower bound for the difference in DP gaps,

$$H(\Theta_0 + \Delta) - H(\Theta_0) \geq - \frac{4\sqrt{g}(\sqrt{\alpha} + \underline{k}^{-1})}{\bar{p}} \sqrt{H(\Theta_0)} \geq - \frac{c_3 g}{\bar{p}} \sqrt{H(\Theta_0)}. \quad (20)$$

We now combine the lower bounds for each term in (12), that is, (17), (18), (19), and (20). For $\epsilon_1 < 1$, we let

$$\mu_1 = \frac{c_1}{\epsilon_1} \sqrt{\frac{\log p}{n}}.$$

Then, we have that

$$\begin{aligned}
G(\Delta) &\geq \frac{1}{2\tau} \underline{k}^2 \|\Delta\|_F^2 - c_1 \sqrt{\frac{\log p}{n}} \|\Delta_{\mathcal{D}}\|_1 - c_2 r_n \|\Delta_{\mathcal{D}}\|_F \\
&\quad + \mu_1 (\|\Delta_{\bar{\mathcal{D}} \cap \mathcal{S}}\|_1 - \|\Delta_{\mathcal{D} \cap \mathcal{S}}\|_1) - \frac{\mu_2 c_3 g}{\bar{p}} \sqrt{H(\Theta_0)} \\
&\geq \frac{1}{2\tau} \underline{k}^2 \|\Delta\|_F^2 - c_1 \left(1 + \frac{1}{\epsilon_1}\right) r_n \|\Delta_{\bar{\mathcal{D}}}\|_F - c_2 r_n \|\Delta_{\mathcal{D}}\|_F - \frac{\mu_2 c_3 g}{\bar{p}} \sqrt{H(\Theta_0)} \\
&= \|\Delta_{\bar{\mathcal{D}}}\|_F \left[\frac{1}{4\tau} \underline{k}^2 \|\Delta_{\bar{\mathcal{D}}}\|_F - c_1 \left(1 + \frac{1}{\epsilon_1}\right) r_n \right] \\
&\quad + \|\Delta_{\mathcal{D}}\|_F \left[\frac{1}{4\tau} \underline{k}^2 \|\Delta_{\mathcal{D}}\|_F - c_2 r_n \right] \\
&\quad + \left[\frac{1}{4\tau} \underline{k}^2 \|\Delta\|_F^2 - \frac{\mu_2 c_3 g}{\bar{p}} \sqrt{H(\Theta_0)} \right], \tag{21}
\end{aligned}$$

$$+ \|\Delta_{\mathcal{D}}\|_F \left[\frac{1}{4\tau} \underline{k}^2 \|\Delta_{\mathcal{D}}\|_F - c_2 r_n \right] \tag{22}$$

$$+ \left[\frac{1}{4\tau} \underline{k}^2 \|\Delta\|_F^2 - \frac{\mu_2 c_3 g}{\bar{p}} \sqrt{H(\Theta_0)} \right], \tag{23}$$

where we aim to find conditions on $\|\Delta\|_F$ ensuring that each term (21), (22), and (23) are positive so that $G(\Delta) > 0$. For the first two terms (21) and (22), we obtain the following lower bounds

$$\|\Delta_{\bar{\mathcal{D}}}\|_F > 4\tau \underline{k}^{-2} c_1 \left(1 + \frac{1}{\epsilon_1}\right) r_n \tag{24}$$

and

$$\|\Delta_{\mathcal{D}}\|_F > 4\tau \underline{k}^{-2} c_2 r_n, \tag{25}$$

respectively. For the third term (23), we have

$$\|\Delta\|_F^2 > 4\tau c_3 \mu_2 \cdot \frac{g}{\bar{p}} \sqrt{H(\Theta_0)}. \tag{26}$$

All three conditions (25), (24), and (26) guarantee that $G(\Delta)$ is positive. Combining the conditions, we obtain a sufficient condition to ensure that $G(\Delta) > 0$,

$$\|\Delta\|_F > \max \left\{ 4\tau \underline{k}^{-2} \left(c_1 \left(1 + \frac{1}{\epsilon_1}\right) + c_2 \right) r_n, \sqrt{4\tau c_3 \mu_2} \cdot \sqrt{\frac{g}{\bar{p}}} \sqrt[4]{H(\Theta_0)} \right\}. \tag{27}$$

Thus, there exist constants $m_1, m_2 > 0$ such that with high probability as $n, p \rightarrow \infty$,

$$\|\Delta\|_F > m_1 r_n + m_2 \frac{\sqrt{g} \sqrt[4]{H(\Theta_0)}}{\sqrt{\bar{p}}}.$$

When this holds for any $\Delta \in \mathcal{M}$, then we have shown that $G(\Delta) > 0$. Thus, since $G(\Delta^*) \leq 0$ and $\Delta^* \in \mathcal{M}$, we have that

$$\|\Delta^*\|_F \leq m_1 r_n + m_2 \frac{\sqrt{g} \sqrt[4]{H(\Theta_0)}}{\sqrt{\bar{p}}}$$

with high probability. Recalling that $g\bar{p} = p$ by AS4, we obtain the inequality in (5), as desired. Moreover, note that if we select μ_2 such that

$$\begin{aligned}
\mu_2 &\leq \frac{4\tau \underline{k}^{-4}}{c_3} \left(c_1 \left(1 + \frac{1}{\epsilon_1}\right) + c_2 \right)^2 \left(\frac{\bar{p}^2 \log p}{n \sqrt{H(\Theta_0)}} \right) \\
&\leq \frac{4\tau \underline{k}^{-4}}{c_3} \left(c_1 \left(1 + \frac{1}{\epsilon_1}\right) + c_2 \right)^2 \left(\frac{\bar{p}(p+s) \log p}{ng \sqrt{H(\Theta_0)}} \right),
\end{aligned}$$

then (27) becomes equivalent to

$$\|\Delta\|_F > 4\tau \underline{k}^{-2} \left(c_1 \left(1 + \frac{1}{\epsilon_1}\right) + c_2 \right) r_n,$$

and we need only satisfy $\|\Delta\|_F > m_1 r_n$ with probability tending to 1 as $n, p \rightarrow \infty$ for any $\Delta \in \mathcal{M}$, which guarantees that $G(\Delta) > 0$. Again, since $G(\Delta^*) \leq 0$, we then have with high probability as $p \rightarrow \infty$ that

$$\|\Delta^*\|_F \leq m_1 r_n$$

for small enough μ_2 dependent on the dimension p , the number of samples n , the number of groups g , and the fairness of the true precision matrix $H(\Theta_0)$, satisfying (7) as desired.

C Proof of Corollary 1

Recall that by definition, $\Theta_0 \Sigma_0 = \mathbf{I}$. Then,

$$\|\Theta^* \Sigma_0 - \mathbf{I}\|_F = \|(\Theta^* - \Theta_0) \Sigma_0\|_F \leq \bar{k} \|\Theta^* - \Theta_0\|_F.$$

The result then follows from Theorem 1 for $m'_1 = \bar{k} m_1$ and $m'_2 = \bar{k} m_2$.

D Optimization Algorithm Details

We provide an overview on computing the update steps for Algorithm 1. For each iteration, we first take a gradient step for $f(\Theta)$, where the Lipschitz constant of f plays the role of the step size, then we perform a proximal step over the non-smooth terms in $h(\Theta)$. The proximal step for $h(\Theta)$ is the soft-thresholding operation for the ℓ_1 norm,

$$\mathcal{T}_\lambda(\Theta_{ij}) = \max\{|\Theta_{ij}| - \lambda, 0\} \text{sign}(\Theta_{ij}),$$

where $\text{sign}(x)$ returns the sign of x . After the proximal gradient step, we perform an orthogonal projection $\Pi_{\mathcal{M}}$ onto the feasible set, which in our case is given by

$$\Pi_{\mathcal{M}}(\Theta) = \mathbf{V} \min \left\{ \max \{ \Lambda, 0 \}, \alpha^{1/2} \right\} \mathbf{V}^\top, \quad (28)$$

with \mathbf{V} and Λ respectively denoting the eigenvectors and eigenvalues of Θ , and with some abuse of notation we let $\min\{\max\{\Lambda, 0\}, \alpha^{1/2}\}$ denote an element-wise minimum and maximum operation on the entries of Λ , which projects all the eigenvalues in the diagonal of Λ onto the interval $[0, \alpha^{1/2}]$.

Both the gradient $\nabla_{\Theta} f$ and the Lipschitz constant L of f are contingent on the choice of bias penalty. The following two lemmas provide their computation for the cases where we apply $R_H = H$, our DP gap measurement (2), or $R_H = H_{\text{node}}$, its node-wise alternative (3). The proofs of both lemmas are deferred to Appendix E.

Lemma 2 *Let the bias penalty R_H in (4) be given by $H(\Theta)$ in (2). Then, the gradient of $f(\Theta)$ is given by*

$$\nabla_{\Theta} f(\Theta) = \hat{\Sigma} - (\Theta + \epsilon \mathbf{I})^{-1} + \frac{2\mu_2}{g^2 - g} \sum_{a=1}^g \sum_{b \neq a} \text{tr}(\mathbf{C}_{ab} \Theta) \mathbf{C}_{ab}^\top \quad (29)$$

where $\mathbf{C}_{ab} := [\mathbf{z}_a \mathbf{z}_a^\top / (p_a^2 - p_a) - \mathbf{z}_a \mathbf{z}_b^\top / (p_a p_b)]_{\mathcal{D}}$ for every $a, b \in [g]$ such that $a \neq b$. Moreover, for $\bar{\mathbf{C}} := \sum_{a \neq b} \mathbf{C}_{ab} \otimes \mathbf{C}_{ab}^\top$ we have that $\nabla_{\Theta} f(\Theta)$ is Lipschitz with constant

$$L_1 = \frac{1}{\epsilon^2} + \frac{2\mu_2}{g^2 - g} \lambda_{\max}(\bar{\mathbf{C}}) \leq \bar{L}_1 = \frac{1}{\epsilon^2} + \frac{2\mu_2}{g^2 - g} \sum_{a=1}^g \sum_{b \neq a} \lambda_{\max}^2(\mathbf{C}_{ab}).$$

Intuitively, while L_1 is a smaller Lipschitz constant, it involves computing the eigendecomposition of a $p^2 \times p^2$ matrix, which may be prohibitive in higher-dimensional settings. Consequently, \bar{L}_1 provides an approximation involving only $p \times p$ matrices. The following lemma provides similar results when the node-wise DP gap H_{node} is employed.

Lemma 3 *Let the bias penalty R_H in (4) be given by $H_{\text{node}}(\Theta)$ in (3). Then, the gradient of $f(\Theta)$ is given by*

$$\nabla_{\Theta} f(\Theta) = \hat{\Sigma} - (\Theta + \epsilon \mathbf{I})^{-1} + 2\mu_2 [\mathbf{A} \Theta_{\mathcal{D}}]_{\mathcal{D}},$$

where

$$\mathbf{A} := \frac{1}{pg(g-1)^2} \sum_{a=1}^g \sum_{b \neq a} \left(\sum_{b \neq a} \frac{\mathbf{z}_a}{p_a} - \frac{\mathbf{z}_b}{p_b} \right) \left(\sum_{b \neq a} \frac{\mathbf{z}_a}{p_a} - \frac{\mathbf{z}_b}{p_b} \right)^\top.$$

Moreover, $\nabla_{\Theta} f(\Theta)$ is Lipschitz with constant

$$L_2 = \frac{1}{\epsilon^2} + 2\mu_2 \lambda_{\max}(\mathbf{A}).$$

E Gradients and Lipschitz Constants

Here, we provide the computation of relevant gradients and Lipschitz constants for f in (10) used in the proposed Algorithm 1. Both the gradient and the Lipschitz constant of f depend on the choice of bias penalty $H(\Theta)$.

E.1 Proof of Lemma 2

First, we rewrite the demographic parity ΔDP in (2) as

$$H(\Theta) = \frac{1}{g^2 - g} \sum_{a=1}^g \sum_{b \neq a} \text{tr}(\mathbf{C}_{ab} \Theta)^2, \quad (30)$$

where \mathbf{C}_{ab} is defined in the statement of Lemma 2. The gradient of H can be obtained as

$$\nabla_{\Theta} H(\Theta) = \frac{2}{g^2 - g} \sum_{a=1}^g \sum_{b \neq a} \text{tr}(\mathbf{C}_{ab} \Theta) \mathbf{C}_{ab}^{\top}, \quad (31)$$

and adding it to the gradient of the remaining terms of $f(\Theta)$, the result follows

$$\nabla_{\Theta} f(\Theta) = \hat{\Sigma} - (\Theta + \epsilon \mathbf{I})^{-1} + \frac{2\mu_2}{g^2 - g} \sum_{a=1}^g \sum_{b \neq a} \text{tr}(\Theta \mathbf{C}_{ab}) [\mathbf{C}_{ab}]^{\top}. \quad (32)$$

Next, to show that the gradient of $f(\Theta)$ is Lipschitz, it suffices to show that its Hessian is bounded. The Hessian $\nabla_{\Theta}^2 f(\Theta)$ can be computed as

$$\nabla_{\Theta}^2 f(\Theta) = (\Theta + \epsilon \mathbf{I})^{-1} \otimes (\Theta + \epsilon \mathbf{I})^{-1} + \frac{2\mu_2}{g^2 - g} \sum_{a=1}^g \sum_{b \neq a} (\mathbf{C}_{ab} \otimes \mathbf{C}_{ab}^{\top}), \quad (33)$$

and it is bounded by

$$\begin{aligned} \|\nabla_{\Theta}^2 f(\Theta)\|_2 &\leq \left\| (\Theta + \epsilon \mathbf{I})^{-1} \otimes (\Theta + \epsilon \mathbf{I})^{-1} \right\|_2 + \frac{2\mu_2}{g^2 - g} \left\| \sum_{a=1}^g \sum_{b \neq a} (\mathbf{C}_{ab} \otimes \mathbf{C}_{ab}^{\top}) \right\|_2 \\ &\leq \frac{1}{\epsilon^2} + \frac{2\mu_2}{g^2 - g} \sum_{a=1}^g \sum_{b \neq a} \lambda_{\max}(\mathbf{C}_{ab}) = L_1. \end{aligned} \quad (34)$$

Moreover, it also follows that

$$\begin{aligned} \|\nabla_{\Theta}^2 f(\Theta)\|_2 &\leq \left\| (\Theta + \epsilon \mathbf{I})^{-1} \otimes (\Theta + \epsilon \mathbf{I})^{-1} \right\|_2 + \frac{2\mu_2}{g^2 - g} \|\bar{\mathbf{C}}\|_2 \\ &\leq \frac{1}{\epsilon^2} + \frac{2\mu_2}{g^2 - g} \lambda_{\max}(\bar{\mathbf{C}}) = \tilde{L}_1. \end{aligned}$$

Consequently, the gradient $\nabla_{\Theta} f(\Theta)$ is Lipschitz with constants $L_1 \leq \tilde{L}_1$.

E.2 Proof of Lemma 3

For the node-based DP gap $H_{\text{node}}(\Theta)$ as in (3), applying standard gradient calculus to compute the gradient and the Hessian of $f(\Theta)$ gives

$$\nabla_{\Theta} f(\Theta) = \hat{\Sigma} - (\Theta + \epsilon \mathbf{I})^{-1} + 2\mu_2 [\mathbf{A} \Theta_{\bar{\mathcal{D}}}], \quad (35)$$

$$\nabla_{\Theta}^2 f(\Theta) = (\Theta + \epsilon \mathbf{I})^{-1} \otimes (\Theta + \epsilon \mathbf{I})^{-1} + 2\mu_2 (\mathbf{I} \otimes \mathbf{A}). \quad (36)$$

Then, the Lipschitz constant is obtained from the following upper bound of the Hessian

$$\|\nabla_{\Theta}^2 f(\Theta)\|_2 \leq (\Theta + \epsilon \mathbf{I})^{-1} \otimes (\Theta + \epsilon \mathbf{I})^{-1} \|_2 + 2\mu_2 \|\mathbf{I} \otimes \mathbf{A}\|_2 \leq \frac{1}{\epsilon^2} + 2\mu_2 \lambda_{\max}(\mathbf{A}) = L_2. \quad (37)$$

F Proof of Theorem 2

Our proof builds over the convergence result for FISTA [34, Thm. 4.4], which establishes that the sequence $\{\Theta^{(k)}\}_{k \geq 1}$ generated by FISTA satisfies the following bound

$$F(\Theta^{(k)}) - F(\Theta^*) \leq \frac{2L \|\Theta^{(0)} - \Theta^*\|_F^2}{(k+1)^2}, \quad (38)$$

where Θ^* is the global minimum of the objective function of (4). This result requires $f(\Theta)$, the smooth components of $F(\Theta)$, to be a convex function with Lipschitz continuous gradient, while $h(\Theta)$, the non-smooth components of $F(\Theta)$, are only required to be convex.

From the expression of $f(\Theta)$ and $h(\Theta)$ in (10) it is clear that both terms of our objective function are convex. Furthermore, from Lemma 2 and Lemma 3 it follows that the gradient of $f(\Theta)$ is Lipschitz continuous when we consider $R_H = H$ or $R_H = H_{\text{node}}$, so the conditions from [34, Thm. 4.4] are met and (38) holds.

Next, we demonstrate that the objective function $F(\Theta)$ is strongly convex. A function $F(\Theta)$ is σ -strongly convex if $F(\Theta) - \sigma \|\Theta\|_F^2$ is also convex, which implies that $\nabla_{\Theta}^2 F(\Theta) - \sigma \mathbf{I} \succeq \mathbf{0}$. Put in words, the eigenvalues of the Hessian need to be larger than σ for $F(\Theta)$ to be σ -strongly convex. Let $f_1(\Theta) = \text{tr}(\hat{\Sigma}\Theta) - \log \det(\Theta + \epsilon \mathbf{I})$, whose Hessian is given by

$$\nabla_{\Theta}^2 f_1(\Theta) = (\Theta + \epsilon \mathbf{I})^{-1} \otimes (\Theta + \epsilon \mathbf{I})^{-1}. \quad (39)$$

Since Θ is constrained by $\|\Theta\|_2^2 \leq \alpha$, applying the properties of the inverse and the Kronecker product renders the following bound on the eigenvalues of $\nabla_{\Theta}^2 f_1(\Theta)$

$$\lambda_{\min}(\nabla_{\Theta}^2 f_1(\Theta)) = \frac{1}{\lambda_{\max}^2(\Theta + \epsilon \mathbf{I})} \approx \frac{1}{\lambda_{\max}^2(\Theta)} = \frac{1}{\alpha}. \quad (40)$$

Recall that ϵ is assumed to be a small parameter such that $\epsilon^2 \ll \lambda_{\max}^2(\Theta)$. Consequently, $\nabla_{\Theta}^2 f_1(\Theta) \succeq \frac{1}{\alpha} \mathbf{I}$, so $f_1(\Theta)$ is strongly convex with constant $\frac{1}{\alpha}$, hence rendering $F(\Theta)$ also strongly convex with the same constant.

The last ingredient is given by [67, Thm. 5.25], which establishes that if $F(\Theta)$ is strongly convex with constant σ , then

$$\|\Theta - \Theta^*\|_F^2 \leq \frac{2}{\sigma} (F(\Theta) - F(\Theta^*)), \quad (41)$$

for every Θ in the domain of F .

Finally, our result follows from combining (38) and (41).

G Experimental Details

The following details include descriptions of our datasets, baselines, and performance metrics. For synthetic experiments, we run simulations over 50 independent realizations of generated data. Moreover, excepting experiments for which we test different specific parameter values, we choose optimal values of hyperparameters via grid search.

Datasets. The numerical evaluation of the proposed algorithm is carried out over synthetic and real-world data. The main features of the different datasets are summarized in Table 3. Additional details are given next.

- **Synthetic data.** Unless specified otherwise, graphs with $p = 100$ nodes are sampled from an Erdős-Rényi (ER) random graph model with an average of 10 links per node. The precision matrix is set to either the combinatorial graph Laplacian [33] or an adjacency matrix with a loaded diagonal to ensure positive definiteness, and is employed to sample graph signals from a zero-mean multivariate Gaussian distribution. The number of sampled signals satisfies the conditions of Theorem 1. For experiments based on synthetic data, 50 independent realizations of graphs and signals are generated and we report the mean performance.

- **Karate club.** A social network where the 34 nodes represent members from a karate club and edges capture interactions between pairs of members outside the club [22, 23]. Since this graph does not have associated nodal observations, we generate signals as multivariate Gaussian samples as described in the previous point for synthetic data using the adjacency matrix of the social network with a loaded diagonal as the precision matrix. Similarly, we evaluate experiments with this synthetic data over 50 independent realizations of generated signals with the mean performance reported.
- **MovieLens**¹. This movie-recommendation dataset contains ratings for 1,682 movies by 943 users, resulting in sparse data as many movies have few ratings. To address this sparsity, we followed the setup in [17] and selected the 200 most-rated movies as nodes, using the ratings from the 943 users as graph signals. Since the dataset lacks a ground truth graph, we report the model fit as defined in Corollary 1 rather than the error in Table 2. The sensitive attribute for each node is determined by whether the movie was released before or after 1991.
- **Co-authorship**². The dataset includes papers from the ACM conference, featuring 17,431 authors, 122,499 papers, and 1,903 keywords. The nodes represent a subset of these authors. To create the ground truth graph, we analyzed author-paper relationships and established an edge between two authors if they collaborated on a paper. For graph data generation, we utilized the total number of different keywords, with each input graph signal reflecting the frequency with which a specific author uses a particular keyword across their papers. We constructed the graph by selecting a connected subset of the authors. The associated graph signals were then used to estimate the graph through the considered methods. The sensitive attribute associated with each author is determined by the conference type in which that author publishes the most.
- **School**³. The dataset contains the temporal network of contacts between students in a high school in Marseilles, France. The data includes the interactions of students from three classes over four days in December 2011. We used the available contact data to construct a ground truth graph, where nodes represent students and edges represent all interactions between them. We generated the signals by grouping the interactions into sets of four. Gender was considered as sensitive attribute for each node.
- **Friendship**⁴. This dataset corresponds to the contacts and friendship relations between students in nine classes at a high school in Marseilles, France, over five days in December 2013. Following the same procedure as with the School dataset, we used the available contact data to generate the ground truth graph, where nodes represent students and edges represent all interactions between them. The graph signals were generated by grouping the interactions into sets of four, and gender was considered the sensitive attribute.

Baselines. We compare the performance of our proposed Fair GLASSO approach with the following baselines:

- **GL:** The celebrated graphical lasso algorithm from [26] constitutes a workhorse alternative to estimate the topology of the graph encoded in precision matrices. However, it ignores the sensitive attributes of the nodes, so it is prone to include biases existing in the true graph.
- **RWGL:** a naive fair alternative to graphical lasso where several edges are randomly rewired after estimating the precision matrix with GL. Since the rewiring process is independent of the sensitive attributes of nodes, it will render a fairer estimate, but the random perturbation may yield highly inaccurate estimates. Methods denoted “**RWGL-N**” for some positive integer N represents **RWGL** with N edges rewired.
- **FST:** a fair alternative for learning the graph from stationary observations while mitigating biases in the topology via a group-wise bias penalty [18, 35]. Different from graphical lasso, stationary methods assume that the covariance of the observed data is a polynomial of a matrix encoding the graph topology. This more lenient assumption typically comes at the expense of requiring a larger number of observations.
- **NFST:** a variant of FST that estimates the graph topology from stationary observations including a node-wise regularization to promote fairness [15, 18].

¹<https://grouplens.org/>

²<https://dl.acm.org/>

³<http://www.sociopatterns.org/datasets/high-school-dynamic-contact-networks/>

⁴<http://www.sociopatterns.org/datasets/high-school-contact-and-friendship-networks/>

	Nodes	Edges	Signals	Groups	Sensitive attribute
School	126	959	28561	2	Gender
Co-authorship	130	525	1903	6	Publication type
MovieLens	200	665	943	2	Old/New
Friendship	311	1009	47127	2	Gender

Table 3: Properties of the real datasets used in Section 4.

Moreover, note that the notation “**FGL-X**” for some number \mathbf{X} denotes **FGL** with $\mu_2 = \mathbf{X}$, and this similarly holds for “**NFGL-X**”.

Performance metrics. To measure the error of our estimated precision matrices Θ^* , we apply the following normalized squared Frobenius error

$$\left\| \frac{[\Theta^*]_{\mathcal{D}}}{\|[\Theta^*]_{\mathcal{D}}\|_F} - \frac{[\Theta_0]_{\mathcal{D}}}{\|[\Theta_0]_{\mathcal{D}}\|_F} \right\|_F^2$$

for true precision matrix Θ_0 . When such a true matrix Θ_0 is unavailable, we instead apply the left-hand side of (8) from Corollary 1 using the sample covariance matrix $\hat{\Sigma}$ estimated from observations.

To measure the bias in a given precision matrix Θ^* for nodal group memberships \mathbf{Z} , observe that H and H_{node} compute average differences in edge weights within and across groups, whether group-wise or node-wise. Thus, for our practical bias metric we normalize by edge weight to obtain

$$\frac{2\sqrt{H(\Theta^*)}}{\|[\Theta^*]_{\mathcal{D}}\|_1},$$

that is, we take the square root of $H(\Theta)$, which acts as a squared ℓ_2 norm across distinct group pairs, and we divide by the average edge weight for unordered variable pairs.

Hardware details. The experiments are run on a computer with AMD Ryzen Threadripper 3970X 32-Core Processor, two Nvidia Titan RTX GPU, and 188GB of RAM.

H Limitations and Future Work

This work focuses on group fairness via minimizing DP gap for Gaussian graphical models. While our proposed definition of DP for graphical models does not require Gaussianity, the theoretical results and optimization algorithm require assuming both Gaussian random variables and use of our proposed metrics. Interesting and critical extensions of this work include more general graphical models and other ideas of fairness. Moreover, while we considered discrete sensitive attributes, we also aim to promote equitable treatment for continuous sensitive traits.

Additional future directions include consideration of more general families of graphs. While we consider the underexplored case of signed, weighted graphs for fairness, our work is specific to graphical models encoding conditional dependence. We aim to consider more general interpretations of graphs with real-valued edges, including the novel extension to directed graphs.